Inorg. Chem. **2005**, *44*, 5745–5752

A Detailed Resonance Raman Spectrum of Nickel(II)-Substituted *Pseudomonas aeruginosa* Azurin

Roman S. Czernuszewicz,* Grazyna Fraczkiewicz, and Adelajda A. Zareba

Department of Chemistry, University of Houston, Houston, Texas 77204-5003

Received April 9, 2005

Nickel(II) and cobalt(II) derivatives of the blue copper protein *Pseudomonas aeruginosa* azurin have been studied by resonance Raman (RR) spectroscopy at liquid-nitrogen temperatures. Vibrational assignments for the observed RR bands of Ni(II)–azurin have been made through a study of ^{62}Ni-substituted azurin. A comparison of Ni(II)–azurin RR spectra with those of the wild type (Cu-containing) protein showed Ni(II)–S(Cys) stretching vibrations, $\nu(\text{Ni–S})_{\text{Cys}}$, at substantially lower frequencies ($\sim$360 versus $\sim$400 cm^{-1}, respectively), indicating that the Ni(II)–S(Cys) bond is much weaker than the corresponding Cu(II)–S(Cys) bond. Resonance enhanced predominantly $\nu(\text{Ni–N})_{\text{His}}$ modes indicate that the metal–N(His) bond distances in the Ni(II) derivative are the same as those in native azurin. The vibrational data also confirm a tetrahedral disposition of ligands about the metal in Ni(II)–azurin found in the protein crystallographic structures. As expected, excitation profile measurements on Ni(II)–azurin show that the $\nu(\text{Ni–S})_{\text{Cys}}$ assignable modes give maxima at the 440-nm absorption band, which confirms a S(Cys) $\rightarrow$ Ni(II) charge-transfer origin of the 440-nm electronic transition in Ni(II)-substituted azurin.

Introduction

Azurin is a small cupredoxin ($\sim$14 kDa) comprising a single polypeptide chain of 128 amino acid residues and one so-called blue or type 1 copper(II) ion.[1−5] In its reduced form, the azurin has been found[6,7] to supply electrons to nitrite reductase, an enzyme that reduces nitrite to nitric oxide under anaerobic conditions in denitrifying bacteria.[8−10] The crystal structures of azurins from several different sources in the oxidized and reduced forms,[6,11−19] the apo form,[20,21] and various site-directed mutants[22−26] have been solved. The azurin molecule consists of a β-barrel structure where the copper ion lies about 7 Å below the surface under a

* Author to whom correspondence should be addressed. E-mail: Roman@uh.edu.

(1) Spiro, T. G. *Copper Proteins*; Wiley: New York, 1981.
(2) Adman, E. T. In *Topics in Molecular and Structural Biology: Metalloproteins*; Harrison, P. M., Ed.; Verlag Chemie: Weinheim, Germany, 1985; Vol. 6, pp 1−42.
(3) Adman, E. T. *Adv. Protein Chem.* **1991**, *42*, 145−197.
(4) Sykes, A. G. *Adv. Inorg. Chem.* **1991**, *36*, 377−408.
(5) Chapman, S. K. In *Perspectives on Bioinorganic Chemistry*; Hay, R. W., Dilworth, J. R., Nolan, K. B., Eds.; Jai Press Ltd.: London, 1991; Vol. 1, pp 95−140.
(6) Dodd, F. E.; Hasnain, S. S.; Hunter, W. N.; Abraham, Z. H. L.; Debenham, M.; Kanzler, H.; Eldridge, M.; Eady, R. R.; Ambler, R. P.; Smith, B. E. *Biochemistry* **1995**, *34*, 10180−10186.
(7) Murphy, L. M.; Dodd, F. E.; Yousafzai, F. K.; Eady, R. R.; Hasnain, S. S. *J. Mol. Biol.* **2002**, *315*, 859−871.
(8) Payne, W. J. In *Denitrification in the Nitrogen Cycle*; Gloterman, H. L., Ed.; Plenum: New York, 1985.
(9) Averill, B. A. *Chem. Rev.* **1996**, *96*, 2951−2964.
(10) Zumft, W. G. *Microbiol. Mol. Biol. Rev.* **1997**, *61*, 533−616.
(11) Adman, E. T.; Jensen, L. H. *Isr. J. Chem.* **1981**, *21*, 8−12.
(12) Nar, H.; Messerschmidt, A.; Huber, R.; van de Kamp, M.; Canters, G. W. *J. Mol. Biol.* **1991**, *221*, 765−772.
(13) Norris, G. E.; Anderson, B. F.; Baker, E. N. *J. Mol. Biol.* **1983**, *165*, 501−521.
(14) Baker, E. N. *J. Mol. Biol.* **1988**, *203*, 1071.
(15) Shepard, W. E. B.; Anderson, B. F.; Lewandowski, D. A.; Norris, G. E.; Baker, E. N. *J. Am. Chem. Soc.* **1990**, *112*, 7817−7819.
(16) Lee, X.; Dahms, T.; Ton-That, H.-W.; Zhu, D. W.; Biesterfeldt, J.; Lanthier, P. H.; Yaguchi, M.; Szabo, A. G. *Acta Crystallogr., Sect. D* **1997**, *D53*, 493−506.
(17) Inoue, T.; Nishio, N.; Kanamoto, K.; Suzuki, S.; Yamaguchi, K.; Kataoka, K.; Tobari, J.; Kai, Y. *Acta Crystallogr., Sect. D* **1999**, *D55*, 307−309.
(18) Li, C. M.; Inoue, T.; Gotowda, M.; Suzuki, S.; Yamaguchi, K.; Kai, K.; Kai, Y. *Acta Crystallogr., Sect. D* **1998**, *D54*, 347−354.
(19) Dodd, F. E.; Abraham, Z. H. L.; Eady, R. R.; Hasnain, S. S. *Acta Crystallogr., Sect. D* **2000**, *D56*, 690−696.
(20) Nar, H.; Messerschmidt, A.; Huber, R.; van de Kamp, M.; Canters, G. W. *FEBS Lett.* **1992**, *306*, 119−124.
(21) Shepard, W. E. B.; Kingston, R. L.; Anderson, B. F.; Baker, E. N. *Acta Crystallogr., Sect. D* **1993**, *D49*, 331−343.
(22) Zumft, W. G.; Gotzmann, D. J.; Kroneck, P. M. H. *Eur. J. Biochem.* **1987**, *168*, 301−307.
(23) Nar, H.; Messerschmidt, A.; Huber, R.; van de Kamp, M.; Canters, G. W. *J. Mol. Biol.* **1991**, *218*, 427−447.
(24) Romero, A.; Hoitink, C. W. G.; Nar, H.; Huber, R.; Messerschmidt, A.; Canters, G. W. *J. Mol. Biol.* **1993**, *229*, 1007−1021.
(25) Tsai, L.-C.; Bonander, N.; Harata, K.; Karlsson, G.; Vänngård, T.; Langer, V.; Sjölin, L. *Acta Crystallogr., Sect. D* **1996**, *D52*, 950−958.
(26) Karlsson, B. G.; Tsai, L.-C.; Nar, H.; Sanders-Loehr, J.; Bonander, N.; Langer, V.; Sjölin, L. *Biochemistry* **1997**, *36*, 4089−4095.

10.1021/ic050553g CCC: $30.25
Published on Web 07/09/2005

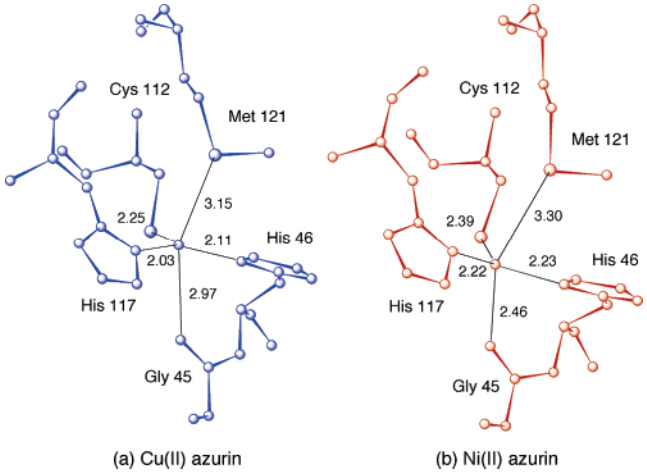

Figure 1. Structural diagrams of the metal site in (a) native (Cu-containing) *Pseudomonas aeruginosa* azurin and (b) its nickel(II) derivative as determined by X-ray crystallography. Data from Nar et al. (Cu−azurin)[12] and Moratal et al. (Ni−azurin).[69]

hydrophobic patch and is strongly coordinated to three equatorial ligands (N^{δ} of His46 and His117 and S^{γ} of Cys112) and weakly coordinated to two axial ligands (S^{δ} of Met121 and carbonyl O of Gly45) (Figure 1a).[6,11−19] This coordination geometry, the carbonyl O excepted, is conserved in all known structures of type 1 Cu sites determined so far, although mutageneses of His46,[27] His117,[28] and Cys112[29] have shown that Cys112 is the only coordinated amino acid that is absolutely essential for a blue Cu center. The type 1 Cu center found in azurin exhibits a very intense ($\epsilon \sim 5.5 \times 10^3$ M^{-1} cm^{-1}) S(Cys) → Cu(II) charge-transfer (CT) absorption near 627 nm, a narrow hyperfine splitting in the Cu(II) electron paramagnetic resonance signal (<100 cm^{-1}), intense multiple resonance Raman (RR) bands around 400 cm^{-1}, a high reduction potential (∼180−780 mV), low protein reorganization energy ($\lambda \sim 0.7$ eV), and facile electron-transfer dynamics.[1−5,30−48]

Replacement of the Cu(II) ion in native and site-directed mutants of cupredoxins with other divalent metal ions such as Mn(II), Zn(II), Ni(II), Co(II), Ru(II), or Cd(II) proved useful in the structural and spectroscopic characterization of type 1 copper sites by a number of different techniques.[27,29,49−74] Single crystals of several zinc(II)-, cadmium(II)-, nickel(II)-, and cobalt(II)-substituted azurins have been obtained and their protein structures and metal coordination

(27) Germanas, J. P.; Bilio, A. J. D.; Gray, H. B.; Richards, J. H. *Biochemistry* **1993**, *32*, 7698−7702.
(28) den Blaauwen, T.; Canters, G. W. *J. Am. Chem. Soc.* **1993**, *115*, 1121−1129.
(29) Mizoguchi, T. J.; Billio, A. J. D.; Gray, H. B.; Richards, J. H. *J. Am. Chem. Soc.* **1992**, *114*, 10076−10078.
(30) Solomon, E. I.; Hare, J. W.; Dooley, D. M.; Dawson, J. H.; Stephens, P. J.; Gray, H. B. *J. Am. Chem. Soc.* **1980**, *102*, 168.
(31) Gewirth, A. A.; Solomon, E. I. *J. Am. Chem. Soc.* **1988**, *110*, 3811−3819.
(32) Solomon, E. I.; Baldwin, M. J.; Lowery, M. D. *Chem. Rev.* **1992**, *92*, 521−542.
(33) Coremans, J. W.; Poluektov, O. G.; Groenen, E. J. J.; Canters, G. W.; Nar, H.; Messerschmidt, A. *J. Am. Chem. Soc.* **1994**, *116*, 3097−3101.
(34) Bonander, N.; Karlsson, B. G.; Vänngård, T. *Biochemistry* **1996**, *35*, 2429−2436.
(35) van Gastel, M.; Canters, G. W.; Krupka, H.; Messerschmidt, A.; de Waal, E. C.; Warmerdam, G. C. M.; Groenen, E. J. J. *J. Am. Chem. Soc.* **2000**, *122*, 2322−2328.
(36) Börger, B.; Gutschank, J.; Suter, D.; Thomson, A. J.; Bingham, S. J. *J. Am. Chem. Soc.* **2001**, *123*, 2334−2339.
(37) Blair, D. F.; Campbell, G. W.; Schoonover, J. R.; Chan, S. I.; Gray, H. B.; Malmström, B. G.; Pecht, I.; Swanson, B. I.; Woodruff, W. H.; Cho, W. K.; English, A. M.; Fry, H. A.; Lum, V.; Norton, K. A. *J. Am. Chem. Soc.* **1985**, *107*, 5755−5766.
(38) Woodruff, W. H.; Dyer, R. B.; Schoonover, J. R. In *Biological Applications of Raman Spectroscopy*; Spiro, T. G., Ed.; John Wiley: New York, 1988; Vol. 3, pp 413−438.
(39) Sanders-Loehr, J. In *Bioinorganic Chemistry of Copper*; Karlin, K. D., Tyeklár, Z., Eds.; Chapman & Hall: New York, 1993; pp 51−63.
(40) Andrew, C. R.; Sanders-Loehr, J. *Acc. Chem. Res.* **1996**, *29*, 365−372.
(41) Qiu, D.; Dasgupta, S.; Kozlowski, P. M.; Goddard, W. A., III; Spiro, T. G. *J. Am. Chem. Soc.* **1998**, *120*, 12791−12797.
(42) Czernuszewicz, R. S.; Fraczkiewicz, G.; Fraczkiewicz, R.; Dave, B. C.; Germanas, J. P. In *Spectroscopy of Biological Molecules*; Merlin, J. C., Turrel, S., Huvenne, J. P., Eds.; Kluwer Academic Publishers: Dordrecht, The Netherlands, 1995; pp 273−276.
(43) Czernuszewicz, R. S.; Dave, B. C.; Germanas, J. P. In *Spectroscopic Methods in Bioinorganic Chemistry*; Solomon, I., Hodgson, K. O., Eds.; American Chemical Society: Washington, DC, 1997; Vol. 692, pp 220−240.
(44) Czernuszewicz, R. S.; Maes, E. M. In *Education in Advanced Chemistry*; Ziolkowski, J. J., Sobota, P., Eds.; University Publishing House: Wroclaw, Poland, 2000; Vol. 7, pp 1−28.
(45) Di Bilio, A. J.; Hill, M. G.; Bonander, N.; Karlsson, B. G.; Villahermosa, R. M.; Malmström, B. G.; Winkler, J. R.; Gray, H. B. *J. Am. Chem. Soc.* **1997**, *119*, 9921−9922.
(46) Skov, L. K.; Pascher, T.; Winkler, J. R.; Gray, H. B. *J. Am. Chem. Soc.* **1998**, *120*, 1102−1103.
(47) Gray, H. B.; Malmström, B. G.; Williams, R. J. P. *J. Biol. Inorg. Chem.* **2000**, *5*, 551−559.
(48) Crane, B. R.; Di Bilio, A. J.; Winkler, J. R.; Gray, H. B. *J. Am. Chem. Soc.* **2001**, *123*, 11623−11631.
(49) McMillin, D. R.; Holwerda, R. A.; Gray, H. B. *Proc. Natl. Acad. Sci. U.S.A.* **1974**, *71*, 1339−1341.
(50) McMillin, D. R.; Rosenberg, R. C.; Gray, H. B. *Proc. Natl. Acad. Sci. U.S.A.* **1974**, *71*, 4760−4762.
(51) Solomon, E. I.; Rawlings, J.; McMillin, D. R.; Stephens, P. J.; Gray, H. B. *J. Am. Chem. Soc.* **1976**, *98*, 8046−8048.
(52) Tennent, D. L.; McMillin, D. R. *J. Am. Chem. Soc.* **1979**, *101*, 2307−2311.
(53) McMillin, D. R.; Morris, M. C. *Proc. Natl. Acad. Sci. U.S.A.* **1981**, *78*, 6567−6570.
(54) Lum, V.; Gray, H. B. *Isr. J. Chem.* **1981**, *21*, 23−25.
(55) Gray, H. B.; Solomon, E. I. In *Copper Proteins*; Spiro, T. G., Ed.; Wiley: New York, 1981; pp 1−39.
(56) Strong, C.; Harrison, S. L.; Wesley, Z. *Inorg. Chem.* **1994**, *33*, 606−608.
(57) Jiménez, H. R.; Salgado, J.; Moratal, J. M.; Morgenstern-Badarau, I. *Inorg. Chem.* **1996**, *35*, 2737−2741.
(58) Di Bilio, A. J.; Chang, T. K.; Malmström, B. G.; Gray, H. B.; Karlsson, B. G.; Nordling, M.; Pascher, T.; Lundberg, L. G. *Inorg. Chim. Acta* **1992**, *198−200*, 145−148.
(59) Vila, A. J. *FEBS Lett.* **1994**, *355*, 15−18.
(60) Salgado, J.; Jiménez, H. R.; Donaire, A.; Moratal, J. M. *Eur. J. Biochem.* **1995**, *231*, 358−369.
(61) Salgado, J.; Jiménez, H. R.; Moratal, J. M.; Kroes, S.; Warmerdam, G. C. M.; Canters, G. W. *Biochemistry* **1996**, *35*, 1810−1819.
(62) Piccioli, M.; Luchinat, C.; Mizoguchi, T. J.; Ramirez, B. E.; Gray, H. B.; Richards, J. H. *Inorg. Chem.* **1995**, *34*, 7−742.
(63) Hill, H. A. O.; Smith, B. E.; Storm, C. B. *Biochem. Biophys. Res. Commun.* **1976**, *70*, 783−790.
(64) Moratal, J. M.; Salgado, J.; Donaire, A.; Jiménez, H. R.; Castells, J. *Inorg. Chem.* **1993**, *32*, 35−3588.
(65) Feiters, M. C.; Dahlin, S.; Reinhammar, B. *Biochim. Biophys. Acta* **1988**, *955*, 250−260.
(66) Nar, H.; Huber, R.; Messerschmidt, A.; Filippou, A. C.; Barth, M.; Jaquinod, M.; van de Kamp, M.; Canters, G. W. *Eur. J. Biochem.* **1992**, *205*, 1123−1129.
(67) Sjölin, L.; Tsai, L.-C.; Langer, V.; Pascher, T.; Karlsson, B. G.; Nordling, M.; Nar, H. *Acta Crystallogr., Sect. D* **1993**, *D49*, 449−457.
(68) Blackwell, K. A.; Anderson, B. F.; Baker, E. N. *Acta Crystallogr., Sect. D* **1994**, *D50*, 263−270.
(69) Moratal, J. M.; Romero, A.; Salgado, J.; Perales-Alarcón, A.; Jiménez, H. R. *Eur. J. Biochem.* **1995**, *228*, 653−657.

geometries determined by X-ray crystallography.[66−71] In these metalloderivatives, the metal center is better described as a distorted tetrahedron, instead of trigonal bipyramidal as in the Cu(II)−azurin, because the metal ion is shifted away from the Met121 sulfur toward the carbonyl O ligand of Gly45 such that the metal−S(Met) distance at ∼3.30 Å must be regarded as a very weak bond (Figure 1b).

RR spectroscopy has been very successful in structural elucidation of the type 1 copper sites[37−44] and model complexes[75−78] because of a strong enhancement of the metal−thiolate stretching vibrations via coupling to the (Cys)S → Cu(II) electronic CT transitions in the visible region. However, in contrast to native type 1 copper proteins, only low-resolution RR spectra have been reported for nickel(II)-substituted derivatives of *Pseudomonas aeruginosa* azurin,[72] *Alcaligens xylosoxidans* azurin II,[74] and *Rhus vernicifera* stellacyanin.[73] In this paper, cryogenic-temperature (77 K) RR spectra with variable-wavelength excitation are reported for laboratory-modified derivatives of *P. aeruginosa* azurin wherein copper(II) has been replaced with nickel(II) or cobalt(II). Vibrational assignments for the observed RR bands of Ni(II)−azurin are made with the aid of ^{58}Ni/^{62}Ni isotope substitution. Differences between the wild-type (WT; Cu-containing) and Ni(II)-substituted proteins are readily detectable by RR spectroscopy. The RR spectrum of Ni(II)−azurin exhibits resonance-enhanced Ni(II)−S(Cys) stretching vibrations, $\nu(\mathrm{Ni-S})_{\mathrm{Cys}}$, substantially shifted to a lower frequency, which indicates that the Ni(II)−S(Cys) bond is much weaker than the corresponding Cu(II)−S(Cys) bond. Resonance-enhanced predominantly $\nu(\mathrm{Ni-N})_{\mathrm{His}}$ modes are also observed and indicate that the metal−N(His) bond distances in Ni(II) derivatives are the same as those in native azurin. The data also suggest a tetrahedral disposition of ligands about the metal in Ni(II)−azurin, in agreement with the protein crystallographic structures. The RR spectrum of the Co(II)-substituted azurin is only preliminary, and it is similar to that of Ni(II)−azurin.

Materials and Methods

Samples of Ni(II)- and Co(II)-substituted azurins from *P. aeruginosa* were prepared by the literature methods.[50] The cloning, expression, isolation, and purification of wild-type azurin were all carried out as described elsewhere.[71,79−81] The copper was then removed by dialysis against 0.1 M KCN in 20 mM tris-HCl, pH 7.2, for 14 days at room temperature. Protein solutions were at a concentration of 10 mg mL^{-1} in a 10 mM MES pH 6.0 buffer. The azurin metalloderivatives were prepared by adding a 5−10-fold excess of metal ions [a solution of cobalt(II) acetate or nickel(II) sulfate] to the apoprotein solution. The metal uptake was allowed to take place overnight at 4 °C. Reconstitution with Ni(II) gave a pale orange solution, while reconstitution with Co(II) resulted in a light blue solution. The Ni(II) and Co(II) azurins were purified by anion-exchange chromatography on a Mono-Q FPLC (Pharmacia) column with 10 mM tris-HCl at pH = 8.8 as a loading buffer. The proteins were eluted with a salt gradient. The electronic spectra of Cu(II), Ni(II), and Co(II) azurins were measured at room temperature using a Cary 50 spectrophotometer (Varian).

The RR spectra were obtained using lines from Coherent Inova K-2 Kr^+ (354.2, 406.7, 413.1, and 647.1 nm), Coherent Inova 90-6 Ar^+ (457.9−514.5 nm), and Liconix 4260 He−Cd (441.6 nm) ion lasers by collecting backscattered photons directly from the surface of a frozen protein solution held in a vacuum on a liquid-N_2-cooled coldfinger. Under this condition, no protein damage was observed, even during prolonged spectral data acquisition at laser powers of 100−200 mW. Details of this sampling technique are presented elsewhere.[82] A conventional scanning Raman instrument equipped with a Spex 1403 double monochromator (with a pair of 1800 grooves/mm gratings) and a Hamamatsu 928 photomultiplier detector was used to record the spectra under the control of a Spex DM3000 microcomputer system.[83] The spectral slit widths were 2 cm^{-1} with 647.4 nm (native Cu azurin) and 5−7 cm^{-1} with all other laser lines (Ni and Co azurins). The spectrometer was advanced in 0.5 cm^{-1} increments with integration times of 1 s for all spectra. Multiple scans (4−6) were averaged to improve the signal-to-noise ratio. To ensure accurate isotope shift measurements, the ^{58}Ni- and ^{62}Ni-labeled proteins were placed side by side on the coldfinger so that the RR data could be collected under the same conditions. The excitation profile studies were made in a frozen solution pellet cooled to 77 K using the 228-cm^{-1} band of ice as the internal standard. Relative intensities of the Ni(II)−azurin RR bands were estimated from the band areas and were corrected for the detector sensitivity and ν^4-law dependence. The slowly slopping baselines were subtracted out from the digitally collected spectra by using LabCalc software (Galactic). IGOR Pro (version 3.12) software (Wave Metrics, Inc.) was used to prepare the spectral figures.

Results and Discussion

Compared in Figure 2 are the electronic absorption spectra obtained at room temperature from solutions of wild-type (Cu-containing) *P. aeruginosa* azurin and its Ni(II)- and Co(II)-substituted metalloderivatives. It is observed that addition of Ni(II) or Co(II) to apoazurin causes the major cysteine-to-metal CT electronic transition to blue shift from 627 nm (Cu−azurin) to 440 (Ni−azurin) and 330 nm (Co−azurin).

(70) Tsai, L.-C.; Sjölin, L.; Langer, V.; Bonander, N.; Karlsson, B. G.; Vänngård, T. *Acta Crystallogr., Sect. D* **1995**, *D51*, 711−717.
(71) Bonander, N.; Vänngård, T.; Tsai, L.-C.; Langer, V.; Nar, H.; Sjölin, L. *Proteins: Struct. Funct. Genet.* **1997**, *27*, 285−395.
(72) Ferris, N. S.; Woodruff, W. H.; Tennent, D. L.; McMillin, D. R. *Biochem. Biophys. Res. Comm.* **1979**, *88*, 288−296.
(73) Musci, G.; Desideri, A.; Morpurgo, L.; Tosi, L. *J. Inorg. Biochem.* **1985**, *23*, 93−102.
(74) Hannan, J. P.; Davy, S. L.; Eady, R. R.; Andrew, C. R. *J. Biol. Inorg. Chem.* **1998**, *3*, 282−291.
(75) Qiu, D.; Kilpatrick, L.; Kitajima, N.; Spiro, T. G. *J. Am. Chem. Soc.* **1994**, *116*, 2585−2590.
(76) Holland, P. L.; Tolman, W. B. *J. Am. Chem. Soc.* **1999**, *121*, 7270−7271.
(77) Randall, D. W.; George, S. D.; Hedman, B.; Hodgson, K. O.; Fujisawa, K.; Solomon, E. I. *J. Am. Chem. Soc.* **2000**, *122*, 11620−11631.
(78) Randall, D. W.; George, S. D.; Holland, P. L.; Hedman, B.; Hodgson, K. O.; Tolman, W. B.; Solomon, E. I. *J. Am. Chem. Soc.* **2000**, *122*, 11632−11648.
(79) Arvidsson, R. H. A.; Nordling, M.; Lundberg, L. G. *Eur. J. Biochem.* **1989**, *179*, 195−200.
(80) Karlsson, B. G.; Pascher, T.; Nordling, M.; Arvidsson, R. H. A.; Lundberg, L. G. *FEBS Lett.* **1989**, *246*, 211−217.
(81) Blaszak, J. A.; McMillin, D. R.; Thornton, A. T.; Tennent, D. L. *J. Biol. Chem.* **1983**, *258*, 9886.
(82) Czernuszewicz, R. S.; Johnson, M. K. *Appl. Spectrosc.* **1982**, *37*, 297−298.
(83) Czernuszewicz, R. S. In *Methods in Molecular Biology*; Jones, C., Mulloy, B., Thomas, A. H., Eds.; Humana Press: Totowa, NJ, 1993; Vol. 17, pp 345−374.

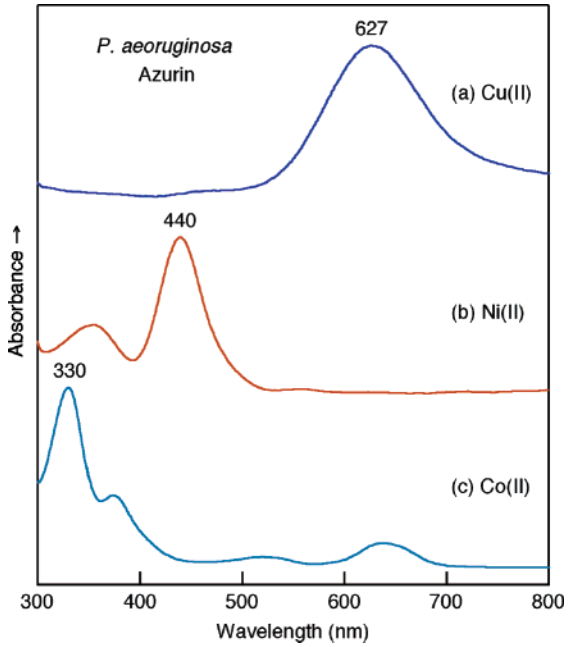

Figure 2. Room-temperature absorption spectra of (a) native *P. aeruginosa* azurin and its (b) Ni(II)- and (c) Co(II)-substituted derivatives.

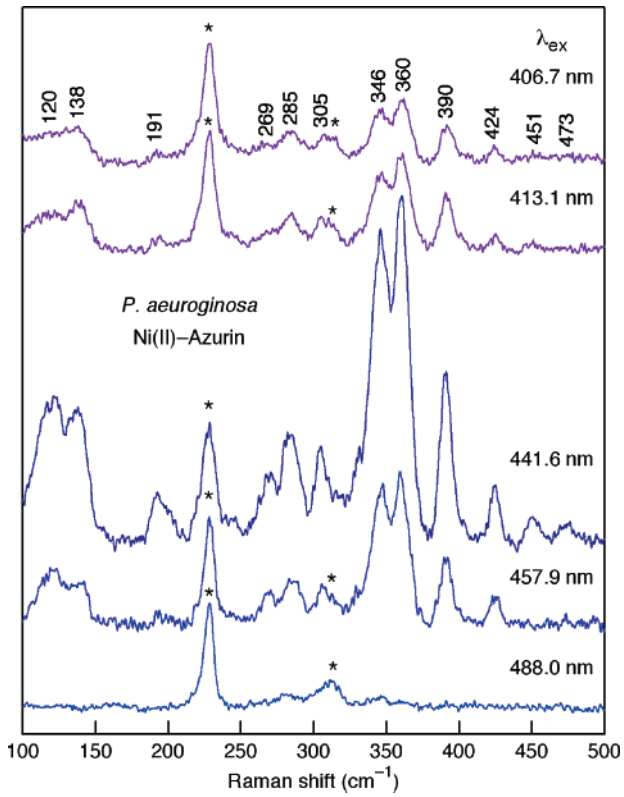

Figure 3. Low-temperature (77 K) RR spectra of Ni(II)-substituted *P. aeruginosa* azurin obtained in the 100−500 cm^{-1} region with indicated excitation wavelengths, ~200 mW laser power (~40 mW for a 441.6 nm line), and 5 cm^{-1} slit widths. Asterisks indicate ice Raman bands.

As a result, pronounced changes are also observed in the RR scattering of Ni(II)− and Co(II)−azurins when the laser excitation is tuned through their absorption bands at 440 and 330 nm, respectively. This is shown in Figure 3, which reports the RR spectra taken in the 100−500 cm^{-1} region from a frozen (77 K) solution of *P. aeruginosa* Ni(II)-

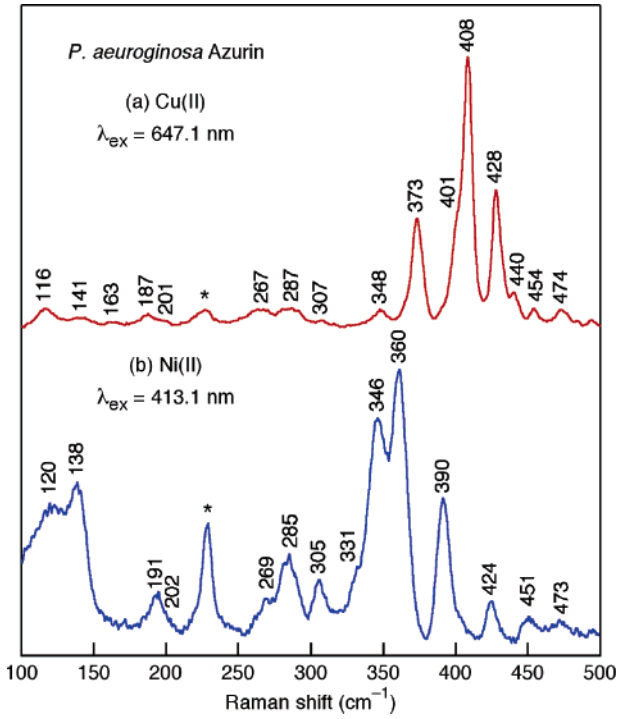

Figure 4. Low-temperature (77 K) RR spectra of *P. aeruginosa* azurin obtained in the 100−500 cm^{-1} region on (a) native Cu(II) protein (647.1 nm excitation wavelength, ~200 mW laser power, and 2 cm^{-1} slit widths) and (b) its Ni(II)-substituted derivative (413.1 nm excitation wavelength, ~200 mW laser power, and 5 cm^{-1} slit widths). Asterisks indicate ice Raman bands.

substituted azurin upon excitation with laser radiation at 406.7, 413.1, 441.6, 457.9, and 488.0 nm, and in Figure 4 where its 413.1-nm excitation spectrum is compared to that of the wild-type protein excited at 647.1 nm. The correlations among the RR bands of native azurin and its Ni(II) derivative are apparent, despite marked frequency and intensity differences. The RR spectra recorded under cryogenic conditions show dramatic improvement in spectral resolution and signal-to-noise ratio, allowing the observation of features that had previously been unnoticed. Table 1 lists the observed RR frequencies for the fundamental vibrations (100−1750 cm^{-1}) of both native *P. aeruginosa* azurin and its Ni(II) derivative, together with those previously reported for Cu(II) and Ni-(II) derivatives of *A. xylosoxidans* azurin II[74] and *R. vernicifera* stellacyanin.[73]

1. Spectral Region 100−500 cm^{-1}. The most obvious finding of the present RR study is that the Ni(II)-substituted azurin gives numerous vibrational bands in the 100−500 cm^{-1} range, which are maximally resonance-enhanced with exciting radiation at 441.6 nm (as judged by the intensity of the protein Raman peaks relative to the ice band; Figure 3) and which uniformly correspond to the vibrational modes of native azurin (Figure 4). A previously published RR spectrum obtained on Ni(II)-substituted *P. aeruginosa* azurin at room temperature[72] exhibits a band at 356 cm^{-1} with an unresolved shoulder at 345 cm^{-1} and a partly obscured by the glass Raman scattering feature at 395 cm^{-1}. Similarly, a room-temperature solution of Ni(II)−azurin II from *A. xylosoxidans* has produced a broad RR band envelope centered near 349 cm^{-1}, which appears to contain contribu-

Table 1. Observed RR Frequencies (cm^{-1}) for Fundamental Vibrational Modes of Native Cu(II) and Ni(II)-Substituted Cupredoxins[a]

Azurin[a] *P. aeruginosa*		Azurin II[b] *A. xylosoxidans*		Stellacyanin[c] *R. vernicifera*		
Cu(II)	Ni(II)	Cu(II)	Ni(II)	Cu(II)	Ni(II)	description[d]
116	120					δ(NMS)
141	138					τ(CC)
163						δ(CCN) + δ(MSC)
187	191					δ(CCC) + δ(OCC)
201 sh	202 sh					δ(CCC) + δ(OCC)
267[e]	269	259		273	275	δ(CCN) + $\nu(MN)_{sym}$
287[e]	285	273		285		$\nu(MN)_{sym}$
307	305			315		$\nu(MN)_{asym}$
348	331 sh	332 sh		349		$\delta(CO)_{ip}$ + δ(CCN)
373	346[f]	375	331 sh	360		δ(CCN) + δ(CCC)
401 sh	**346**[f]	**400**		**376**	**350**	ν(MS) + δ(CCN)
408[g]	**360**	**412**	**349**	**387**	**376**	ν(MS) + δ(SCC)
428	390	426	366	418		δ(CCC) + ν(MS)
440	424			423		δ(OCC) + δ(CCC)
454	451	463		447	454	δ(OCC) + δ(CCC)
474	473			463	467	δ(CCN)
494	493			488		δ(CCN)
520						δ(CCO)
568						δ(CCN)
631	626					amide IV
657	654	654				amide VI
690	693					amide IV + VI
743 sh	750 sh					$\delta(CO)_{wag}$ + ν(CS)
751	**763**	**750**	**755**		**762**	ν(CS)
	828					CH_2 rock
846 sh	842					amide V
900	897					amide V
932	933					amide V
974	962					$\nu(CC_\alpha)$
1001	1000					$\nu(C_\alpha C_\beta)$
1033	1045[f]					$\nu(C_\alpha C_\beta)$
1067	1068					$\nu(C_\alpha C_\beta)$ + $\nu(C_\alpha N)$
1123						$\nu(C_\alpha N)$ + $\nu(C_\alpha C_\beta)$
1150 sh	1147					$\nu(C_\alpha N)$
1193 sh	1198					amide III
1224	**1229**					amide III + CH bend
1243 sh	1252					amide III
1272 sh	1275					CH_2 twist
1300	1301					CH bend
1313	1312					CH bend + CH_2 wag
1344	1350					CH bend + CH_2 wag
	1391					CH_2 scissor
1406	**1417**					CH_2 scissor
1433	1432					amide II
1450	1449					amide II
	1462					amide II
1504	1510					amide II
1529	1533					amide II
1589	1588					amide I
1631	1622					amide I
1650	1643					amide I
1678	1682					amide I

[a] This work. [b] Native and Ni(II) azurin II data from Hannan et al.[74] [c] Native and Ni(II) stellacyanin data from Musci et al.[73] [d] Assignments based on NCA calculations of *P. aeruginosa* azurin.[85] [e] Boldface numbers indicate the RR peak(s) with the greatest intensity; sh = shoulder. [f] Possibly overlapping bands. [g] Contain contributions from peaks at 262/268 and 280/286 cm^{-1}, respectively.

tions from four overlapping peaks at 331, 344, 353, and 366 cm^{-1}.[74] However, when the *P. aeruginosa* Ni(II)−azurin is examined in frozen solutions at liquid-N_2 temperatures without a glass cover,[82] the RR features in this spectral region are now resolved into three sharp peaks at 346, 360, and 390 cm^{-1}, although the 346 cm^{-1} peak is somewhat broader than the other two peaks. Thus, the major vibrations that are observed for the nickel(II) azurin include a group of three intense RR peaks at 346, 360, and 390 cm^{-1} (Figure 4b), which clearly correspond to the strongest RR peaks at 373, 401(sh), 408, and 428 cm^{-1} of the native copper(II) azurin (Figure 4a). Similarly, Co(II)-substituted azurin also gave three bands at 340, 362, and 392 cm^{-1} upon preresonant excitation at 354.2 nm (spectrum not shown). Additional vibrational information in the Ni(II)-substituted azurin RR spectrum, compared to those previously published,[72−74] includes a rich array of moderate-intensity RR bands located below 340 cm^{-1} (331 sh, 305, 285, 269, 245, 202 sh, 191, 138, and 120 cm^{-1}) and above 400 cm^{-1} (424, 451, and 473 cm^{-1}), each band having a counterpart of similar frequency in the Cu(II)−azurin spectrum (Figure 4 and Table 1). Hence, essentially all of the 100−500 cm^{-1} vibrational modes that are observed for the native Cu(II)−azurin have now also been detected in its Ni(II) derivative, allowing for a better understanding of their respective metal sites.

Raman excitation into the (Cys)S → Cu(II) (627 nm) or (Cys)S → Ni(II) (440 nm) CT absorption band of metalloazurin is expected to enhance M−S(Cys) vibrational modes, since the M−S(Cys) bonds are weakened in the CT excited state. Indeed, the Cu−thiolate vibrational origin of the *P. aeruginosa* azurin RR spectrum has been established by examining its sensitivity to the labeling of azurin with isotopes of copper, sulfur, nitrogen, and hydrogen, carried out via bacterial expression of the azurin gene[42−44,84] and by normal coordinate analysis (NCA) calculations carried out on a 34-atom molecular fragment of the azurin active site consisting of Cu, His46, and 117 imidazoles (67 Da point masses) and atoms of Cys112, Phen110, Phen111, and Thr113.[85] The normal mode eigenvectors indicate that the multiple vibrational features arise from kinematic coupling between Cu−S(Cys) stretching motions and heavy atom bending motions of at least four amino acids, Cys112 and Thr113, Phe111, and Phe110 linked to Cys112 in the polypeptide chain. The strongest RR peak of WT azurin, observed at 408 cm^{-1} (Figure 4a), contains the greatest Cu−S(Cys) character (∼40%), because it shifted the most to a lower frequency upon {^{32}S/^{34}S}Cys and ^{63}Cu/^{65}Cu isotope substitution, ∼4.0 and 1.0 cm^{-1}, respectively; the other three prominent peaks in this region (373, 401 sh, 428 cm^{-1}) shifted appreciably less, ∼1.0−2.5 and ∼0.4−0.6 cm^{-1}, respectively.[43,44,84] Thus, to a first approximation, the most intense azurin fundamental peak at 408 cm^{-1} is ascribed to the Cu−S(Cys) stretch, $\nu(Cu-S)_{Cys}$. Although {^{34}S}Cys isotopic shifts are not available for Ni(II)-substituted derivative, the apoprotein samples of *P. aeruginosa* azurin were reconstituted with different Ni isotopes (^{58}Ni or ^{62}Ni) and their high-resolution RR spectra were recorded under identical excitation conditions to provide evidence for a $\nu(Ni-S)_{Cys}$ vibration. Expanded spectra of the low-frequency region are shown in Figure 5. It is observed that, upon substitution of ^{62}Ni for ^{58}Ni, the peaks at 424, 390, 360, 346, 285, and 269 cm^{-1} undergo shifts of −0.4, −1.0, −2.0, −0.8, −1.6, and −1.4 cm^{-1}, respectively. Thus, all of these RR bands

(84) Dave, B. C.; Germanas, J. P.; Czernuszewicz, R. S. *J. Am. Chem. Soc.* **1993**, *115*, 12175−12176.
(85) Fraczkiewicz, R. Ph.D. Dissertation, University of Houston, 1996.

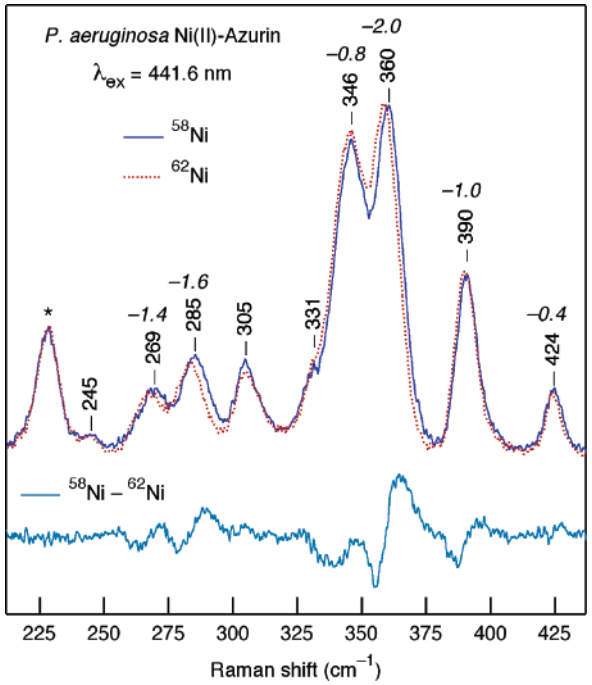

Figure 5. Effects of Ni-isotope substitution on the 200−430 cm^{-1} RR spectrum of *P. aeruginosa* azurin: *top*, apoazurin reconstituted with ^{58}Ni (solid line) or ^{62}Ni (dashed line) and *bottom*, the corresponding (^{58}Ni − ^{62}Ni) difference spectrum. Spectra were recorded at 77 K using 441.6 nm excitation, ∼40 mW laser power, and 5 cm^{-1} slit widths. Asterisks indicate ice Raman bands. Italic numbers show $\{\nu(^{58}Ni) - \nu(^{62}Ni)\}$ band shifts.

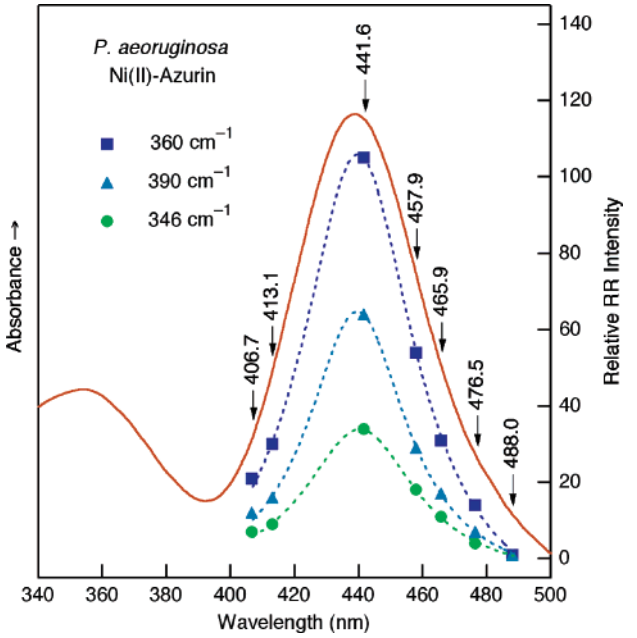

Figure 6. Excitation profiles of *P. aeruginosa* Ni(II)−azurin in a frozen protein solution (77 K) superimposed on the room-temperature electronic absorption spectrum. Raman band intensities were determined relative to the 228 cm^{-1} ice band and normalized to the intensities at the excitation wavelength 488.0 nm.

must arise from vibrational motions that have nickel−ligand oscillatory character. The strongest Ni(II)−azurin band at 360 cm^{-1}, which exhibits the largest isotope shift (−2 cm^{-1}) upon substitution of ^{58}Ni for ^{62}Ni, is ascribed to the predominantly Ni(II)−S(Cys) stretching mode, $\nu(Ni-S)_{Cys}$, analogous to the dominant 408 cm^{-1} $\nu(Cu-S)_{Cys}$ mode in the native azurin. The $\nu(Ni-S)_{Cys}$ character is also detected for the bands at 346 and 390 cm^{-1} from their $^{62/58}Ni$ isotope shifts (−0.8 and −1.0 cm^{-1}, respectively), which is consistent with the kinematic coupling of the metal−thiolate stretch with internal vibrations of the cysteine ligand side chain observed in the RR spectra of cupredoxins and iron−sulfur proteins.[39,40,42−44,86,87] Meanwhile, the frequency of the β-carbon−sulfur(Cys) stretching vibration, $\nu(C-S)_{Cys}$, increased from 751 cm^{-1} in Cu(II)−azurin to 763 cm^{-1} in Ni(II)−azurin (Table 1; Figure 7). Taken together, these vibrational results indicate that Ni(II) substitution causes a significant weakening of the metal−S(Cys) bond as the metal coordination changes from trigonal bipyramidal in Cu(II)−azurin to tetrahedral in Ni(II)-modified protein. This bond weakening is supported by the trend found in X-ray crystallographic studies of *P. aeruginosa* azurin and its Ni(II) derivative, which showed a much longer Ni−S(Cys) bond distance (2.39 Å) in Ni(II)−azurin than in the native protein (2.25 Å) (Figure 1).[12,69]

The present excitation wavelength-dependent RR spectra (Figure 3) also provide unambiguous evidence for the nature of the CT electronic transition at 440 nm due to (Cys)S → Ni(II).[52] Figure 6 compares the Ni(II)−azurin optical absorption spectrum with excitation profiles for the three most intense $^{58/62}Ni$-sensitive RR bands at 346, 360, and 390 cm^{-1}. The profiles are quite similar and closely track the absorption band in the violet region.

In cupredoxins, the vibrations of the $His_2Cu(II)$ moiety occur in the 250−305 cm^{-1} region,[37,43,44,88,89] and Ni-isotope-sensitive RR bands are observed at similar frequencies for Ni(II)-substituted *P. aeruginosa* azurin (Figures 4 and 5, Table 1), implying that Ni(II)−N(His) and Cu(II)−N(His) bond strengths are comparable. This finding appears to disagree with the X-ray structures of Cu(II)− and Ni(II)−azurins as judged by the mean metal−N(His) bond distances of 2.07 and 2.22 Å, respectively (Figure 1).[12,69]

2. Spectral Region 500−1750 cm^{-1}. As Figures 7 (500−1000 cm^{-1}) and 8 (1000−1750 cm^{-1}) show, the RR spectrum of the Ni(II)-substituted *P. aeruginosa* azurin obtained above 500 cm^{-1} is also considerably different than that of the native protein. For Cu(II)−azurin, the region from 500 to 1000 cm^{-1} (Figure 7a) primarily exhibits the overtones and combination modes of the ∼400 cm^{-1} fundamental vibrations, as expected for RR scattering. Another prominent feature in this region is the strongly enhanced $\nu(C_\beta-S)_{Cys}$ vibrational mode of the Cys112 side chain residue, at 751 cm^{-1} in native Cu(II)−azurin. That the 751 cm^{-1} band of *P. aeruginosa* azurin belongs to the cysteine C_β−S stretching vibration has been verified by its observed and calculated −2 cm^{-1} ^{34}S and −50 cm^{-1} $\{C_\beta D_2\}$Cys isotope shifts.[44,85,90] A similar RR band is

(86) Spiro, T. G.; Czernuszewicz, R. S.; Han, S. In *Biological Applications of Raman Spectroscopy*; Spiro, T. G., Ed.; Wiley-Interscience: New York, 1988; Vol. 3, pp 523−553.
(87) Spiro, T. G.; Czernuszewicz, R. S. In *Bioinorganic Spectroscopy and Magnetism*; Que, L., Jr., Ed.; University Science Books: Sausalito, CA, 2000; pp 59−119.
(88) Dong, S.; Spiro, T. G. *J. Am. Chem. Soc.* **1998**, *120*, 10434−10440.
(89) Han, J.; Adman, E. T.; Beppu, T.; Codd, R.; Freeman, H. C.; Huq, L.; Loehr, T. M.; Sanders-Loehr, J. *Biochemistry* **1991**, *30*, 10904−10913.

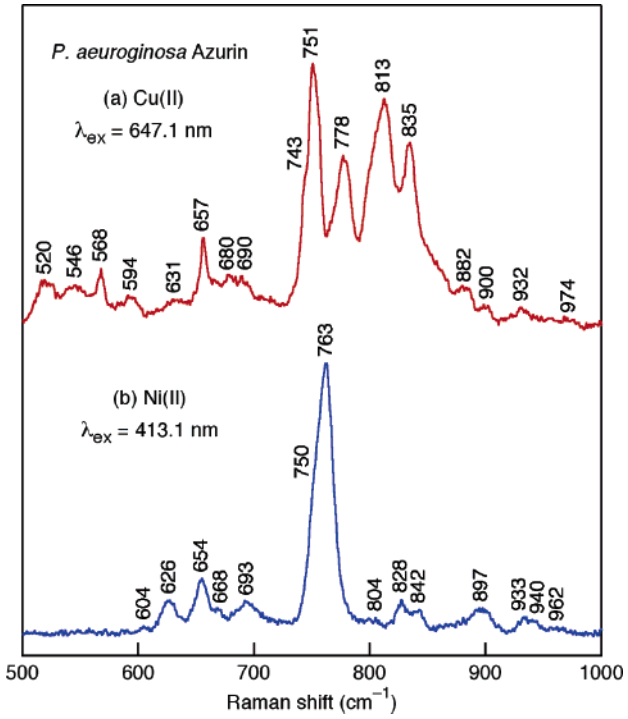

Figure 7. Low-temperature (77 K) RR spectra of *P. aeruginosa* azurin obtained in the 500−1000 cm^{-1} region on (a) native Cu(II) protein (647.1 nm excitation wavelength, ~200 mW laser power, and 2 cm^{-1} slit widths) and (b) its Ni(II)-substituted derivative (413.1 nm excitation wavelength, ~200 mW laser power, and 5 cm^{-1} slit widths).

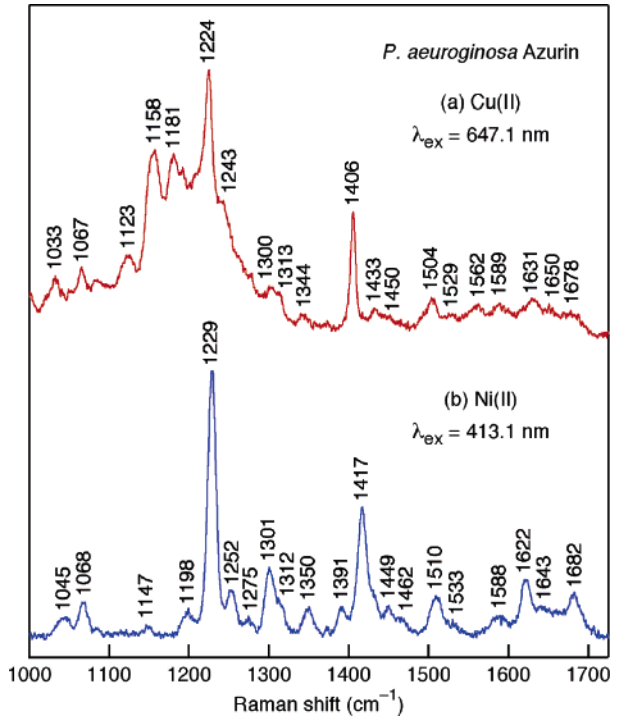

Figure 8. Low-temperature (77 K) RR spectra of *P. aeruginosa* azurin obtained in the 1000−1750 cm^{-1} region on (a) native Cu(II) protein (647.1 nm excitation wavelength, ~200 mW laser power, and 2 cm^{-1} slit widths) and (b) its Ni(II)-substituted derivative (413.1 nm excitation wavelength, ~200 mW laser power, and 5 cm^{-1} slit widths).

seen for the Ni(II)-substituted azurin at 763 cm^{-1} (Figure 7). The increased frequency of this vibration provides additional evidence for reduced Ni(II)−S(Cys) interaction in the Ni(II) derivative. The $\nu(C_\beta-S)_{Cys}$ stretch of Cu(II)−azurin forms its own series of combination modes with the intense ~400-cm^{-1} fundamentals, which appear as weak bands between 1120 and 1220 cm^{-1} (Figure 8a). The remaining bands between 720 and 900 cm^{-1} all fit either overtone or combination frequencies of the four strong fundamentals observed in the 400 cm^{-1} region, and the most intense band at ~813 in the Cu(II)−azurin spectrum is assigned to the first overtone of the predominantly $\nu(Cu-S)_{Cys}$ mode.[42,43] All these bands vanish upon substitution of azurin with Ni(II) in place of Cu(II) and are replaced by a very weak broad envelope near 700 cm^{-1} and an unresolved shoulder at ~750 cm^{-1} (Figure 7b), which are likely to contain combination bands involving the 360 cm^{-1} $\nu(Ni-S)_{Cys}$ fundamental as a progressive mode. No overtone bands of the 346−390 cm^{-1} fundamentals can be identified in the Ni(II)−azurin RR spectrum. This trend toward "disappearing overtones" while combinations persist[91,92] also suggests a pronounced structural distortion in the (Cys)S → Ni(II) CT excited state of the Ni(II)−azurin.[43]

Additional differences between Cu(II) and Ni(II) *P. aeruginosa* azurins occur in the region above 1000 cm^{-1}. A distinct band at 1406 cm^{-1} in the WT azurin spectrum (Figure 8a), which displayed a −289 cm^{-1} shift upon $\{C_\beta D_2\}$Cys incorporation, belongs to the $\rho_s(C_\beta H_2)$ scissors mode of methylene hydrogens on the cysteine 112 β carbon.[44,85] Surprisingly, the frequency of this mode is found to be increased to 1417 cm^{-1} by reconstitution of *P. aeruginosa* apoazurin with Ni(II) (Figure 8b). Another characteristic Cu(II)−azurin RR band in this subregion occurs at 1224 cm^{-1} (Figure 8a). It has been assigned to the cysteine amide III vibration coupled to the C_α hydrogen bending on the basis of its shift to ~1207 cm^{-1} in the $\{C_\beta D_2\}$Cys spectrum and NCA calculations.[85] As Figure 8b shows, Ni(II)−azurin produces this band at a higher (1229 cm^{-1}) frequency. It is clear from the band assignments and spectral changes discussed above that the changes in the metal site structure on replacing Cu(II) with Ni(II) extend beyond the first metal coordination sphere.

Conclusions

In this study, we utilized cryogenic-temperature (77 K) RR spectroscopy to characterize nickel(II)- and cobalt(II)-substituted azurins from *Pseudomonas aeruginosa*. The Ni(II) derivative has been studied in detail over the 100−1800 cm^{-1} spectral region, including $^{58/62}$Ni isotope frequency shift and excitation profile measurements. Substantial weakening of the M(II)−S(Cys) interactions on replacing Cu(II) with Ni(II) and Co(II) is indicated by the downshifted (~40 cm^{-1}) RR bands involving the $\nu(Ni-S)_{Cys}$ and $\nu(Co-S)_{Cys}$ stretching modes, respectively, and the shift from 751 cm^{-1} in Cu(II)−azurin to 763 cm^{-1} in the Ni(II)−azurin $\nu(C_\beta-S)_{Cys}$

(90) Fraczkiewicz, G.; Fraczkiewicz, R.; Germanas, J. P.; Czernuszewicz, R. S. *Proc. XV-th Int. Conf. Raman Spectrosc.*; John Wiley & Sons: Pittsburgh, PA, 1996.
(91) Heller, E. J. *Acc. Chem. Res.* **1981**, *14*, 368.
(92) Heller, E. J.; Sundberg, R. L.; Tannor, D. *J. Phys. Chem.* **1982**, *86*, 1822−1833.

stretching band. A comparison of the predominantly ν(Cu−N)$_{His}$ and ν(Ni−N)$_{His}$ stretching RR bands indicates that the azurin Cu(II)−His and Ni(II)−His bond strengths are nearly identical. The vibrational data also implies a tetrahedral disposition of ligands about the metal in Ni(II)−azurin, in agreement with the protein crystallographic structures. Excitation profile studies on Ni(II)−azurin show that the three most intense $^{58/62}$Ni-sensitive vibrations (346, 360, and 390 cm^{-1}) give maxima at the 440-nm absorption band and provide experimental evidence for its (Cys)S → Ni(II) CT origin. An analysis of the overtone and combination RR bands (500−1200 cm^{-1}) suggests different geometries for the (Cys)S → Cu(II) (627 nm) and (Cys)S → Ni(II) (440 nm) CT excited states.

Acknowledgment. We thank the Robert A. Welch Foundation (Grant E-1184 to R.S.C.) for financial support. Special thanks go to Professor Tore Vänngård and Dr. Nicklas Bonander at Göteborg University and Chalmers University of Technology, Sweden, for their generous gift of the initial samples of Ni(II) and Co(II) *Pseudomonas aeruginosa* azurins.

IC050553G